

DRD2 Genotype-Based Variation of Default Mode Network Activity and of Its Relationship With Striatal DAT Binding

Fabio Sambataro¹, Leonardo Fazio², Paolo Taurisano³, Barbara Gelao³, Annamaria Porcelli³, Marina Mancini³, Lorenzo Sinibaldi², Gianluca Ursini³, Rita Masellis³, Grazia Caforio³, Annabella Di Giorgio³, Artor Niccoli-Asabella⁴, Teresa Popolizio², Giuseppe Blasi³, and Alessandro Bertolino^{*,2,3}

¹Brain Center for Motor and Social Cognition, Istituto Italiano di Tecnologia@UniPr, Parma, Italy; ²Istituto di Ricovero e Cura a Carattere Scientifico, Casa Sollievo della Sofferenza, San Giovanni Rotondo, Italy; ³Psychiatric Neuroscience Group, Department of Neurological and Psychiatric Sciences, University of Bari, “Aldo Moro,” Piazza G. Cesare 11, 70124 Bari, Italy; ⁴Nuclear Medicine Unit, Department of Internal Medicine and of Public Medicine, University of Bari, Bari, Italy

*To whom correspondence should be addressed; tel: +39-080-5478572, fax: +39-080-5593204, e-mail: a.bertolino@psichiatria.uniba.it

The default mode network (DMN) comprises a set of brain regions with “increased” activity during rest relative to cognitive processing. Activity in the DMN is associated with functional connections with the striatum and dopamine (DA) levels in this brain region. A functional single-nucleotide polymorphism within the dopamine D2 receptor gene (*DRD2*, *rs1076560* G > T) shifts splicing of the 2 D2 isoforms, D2 short and D2 long, and has been associated with striatal DA signaling as well as with cognitive processing. However, the effects of this polymorphism on DMN have not been explored. The aim of this study was to evaluate the effects of *rs1076560* on DMN and striatal connectivity and on their relationship with striatal DA signaling. Twenty-eight subjects genotyped for *rs1076560* underwent functional magnetic resonance imaging during a working memory task and 123 55 I-Fluoropropyl-2-beta-carbomethoxy-3-beta(4-iodophenyl) nortropan Single Photon Emission Computed Tomography (¹²³I)-FP-CIT SPECT) imaging (a measure of dopamine transporter [DAT] binding). Spatial group-independent component (IC) analysis was used to identify DMN and striatal ICs. Within the anterior DMN IC, GG subjects had relatively greater connectivity in medial prefrontal cortex (MPFC), which was directly correlated with striatal DAT binding. Within the posterior DMN IC, GG subjects had reduced connectivity in posterior cingulate relative to T carriers. Additionally, *rs1076560* genotype predicted connectivity differences within a striatal network, and these changes were correlated with connectivity in MPFC and posterior cingulate within the DMN. These results suggest that genetically determined D2 receptor signaling is associated with DMN connectivity and that these changes are correlated with striatal function and presynaptic DA signaling.

Key words: *DRD2*/dopamine/default mode network/functional magnetic resonance imaging/single-photon emission computerized tomography

Introduction

Connectivity is a crucial functional property of the brain. Several networks have been described in the brain and these observations have been confirmed across multiple subjects (see also National Institutes of Health’s human connectome project <http://www.humanconnectomeproject.org/>). Recently, much interest has been focused on the default mode network (DMN). The DMN is a large-scale interacting brain system which includes a set of brain regions whose activity increases during rest and is attenuated during an active task, thus resulting in greater task induced deactivations as revealed by classical univariate analyses.¹ Anatomically, this circuit includes midline areas organized in an anterior “hub,” which is localized in the medial prefrontal cortex (MPFC), and a posterior hub encompassing the posterior cingulate cortex (PCC) and the precuneus; lateral areas include bilateral inferior parietal lobule and medial temporal lobes.² The DMN functionally interacts with other brain networks including striatal and task-related networks modulating cognitive and emotional processing.^{3,4} Different roles have been hypothesized for the DMN ranging from monitoring of external environment (watchfulness),⁵ to internal mentation.² Interestingly, midline areas are implicated in emotional and self-referential processing² as well as in the allocation of attentional resources needed for cognitive processing.⁶ Alterations of DMN function have been implicated in severe neuropsychiatric disorders, including schizophrenia.⁷

Evidence suggests that dopamine (DA) levels regulate activity in the DMN network. Pharmacological studies with dopaminergic nonselective agonists, such as apomorphine,⁸ L-DOPA,^{4,9} methylphenidate,¹⁰ and modafinil¹¹ as well as with DA depletion¹² have suggested that DA levels can modulate deactivation of DMN regions. Also, unmedicated patients with Parkinson’s disease

fail to deactivate the DMN during executive function,¹³ and this ability is restored by acute administration of L-DOPA.¹⁴ Consistently, other reports have indicated that genetic variation of the DA-inactivating enzyme catechol-O-methyltransferase affects DMN response.^{15,16} Additionally, striatal markers of DA activity as evaluated with radiotracer imaging techniques have been correlated with DMN activity.^{17,18} Furthermore, functional connectivity between prefrontal cortex (PFC) and striatal regions is suppressed by acute DA depletion resulting in impaired cognitive performance.¹² Consistently, administration of L-DOPA modulates functional coupling between ventral and dorsal striatum and DMN regions.⁴

A crucial determinant of DA signaling is the D2 receptor. Although both D1 and D2 pathways modulate the tuning of cortical neuronal resources, D2 receptors are critically involved in inhibitory processes,¹⁹ which underlie the DMN. The administration of D2 agonists and antagonists, respectively, reduce and increase activity in PFC and striatum during cognitive processing.^{20,21} Also, D2 receptors modulate functional connectivity within brain networks in normal controls.²² Interestingly, D2 signaling has been associated with schizophrenia-related cognitive and imaging phenotypes and response to antipsychotic treatment.^{23,24} D2 receptors have 2 alternatively spliced isoforms, the short (D2S), which is mainly presynaptic acting as an autoreceptor, and the long (D2L), which is primarily postsynaptic. Interestingly, rapid reuptake of DA by dopamine transporter (DAT), that is, one of the key mechanisms for regulation of striatal DA level, is also modulated by presynaptic D2 receptors.²⁵ Activation of D2S can facilitate cell-surface DAT expression through a direct protein-protein interaction modulated by an extracellular signal-regulated kinases 1- and 2-dependent phosphorylation mechanism,²⁶ thus leading to increased DA uptake.²⁵ Also, we have demonstrated in vivo D2S-DAT genetic interaction in mice and in humans.²⁷ Phenotypically, disruption of D2S-DAT interaction in mice using interfering peptides results in increased spontaneous locomotor activity, similar to DAT knockout animals.²⁵ Recently, an association between relative expression of these isoforms and a functional intronic single-nucleotide polymorphism within the gene encoding D2 receptors (*DRD2 rs1076560* G > T) has been identified. Healthy individuals homozygous for the G allele, which have been associated with greater PFC efficiency during cognitive processing,²³ have relatively greater striatal and prefrontal mRNA expression of D2S²⁸ as well as increased in vivo striatal binding of [¹²³I]-FP-CIT,²⁹ which is a SPECT radioligand reflecting the availability of presynaptic DATs.

In the present study, we investigated the relationship between *DRD2 rs1076560* genotype and DMN activity using a multimodal imaging approach. We used blood oxygen level-dependent (BOLD) functional magnetic resonance imaging (fMRI) during a working memory (WM) task to estimate brain connectivity patterns and [¹²³I]-FP-CIT SPECT to measure pre-synaptic DA

signaling in healthy controls. Given the well-known modulation of DA on DMN and the effects of this polymorphism on PFC and striatal DA function, we hypothesized that *DRD2* genotype would be associated with modulation of connectivity strength within the DMN and the striatum. Also, we hypothesized that *DRD2* genotype-dependent connectivity changes in these networks would be predicted by striatal binding of [¹²³I]-FP-CIT.

Methods

Subjects

Twenty-eight right-handed Caucasian subjects (mean age \pm SD = 23.8 \pm 3.2 years) participated in this study (table 1). All subjects had normal or corrected to normal visual acuity. Handedness was assessed with the Edinburgh Questionnaire. Exclusion criteria included past history or the presence of any medical, neurological, or psychiatric disorders according to *Diagnostic and Statistical Manual of Mental Disorders, Fourth Edition*, drug treatment (except birth control pills in women), past head trauma with loss of consciousness. All participants gave written informed consent, approved by the Institutional Review Board of the University of Bari, Bari (Italy), to take part in the experiment. Subjects were genotyped for *DRD2 rs1076560* and the variable number of tandem (VNTR) repeat polymorphism in the 3'-untranslated region of *DAT* (see supplementary materials).

fMRI Imaging Acquisition

BOLD-fMRI was performed on a GE Signa (Milwaukee, WI) 3T scanner. A gradient echo BOLD echo-planar imaging pulse sequence was used to acquire 120 images. Each functional image consisted of 20 6-mm-thick axial slices covering the entire cerebrum and most of the cerebellum (time repetition = 2000 ms; time echo = 30 ms; field-of-view = 24 cm; flip angle = 90°; matrix = 64 \times 64).

fMRI Task Paradigm

All subjects performed the N-back WM task as described elsewhere.²⁹ Briefly, subjects saw numbers (1–4) shown in pseudorandom sequence and displayed at the corners of a diamond-shaped box. A visual-motor control condition (0-back) that required subjects to identify the number currently seen, alternated with the 2-back WM condition. In the 2-back condition, subjects were asked to recall the number seen 2 stimuli before, while continuing to encode additionally incoming stimuli. Performance was recorded through a fiber optic response box, which allowed measurement of behavioral data as the number of correct responses (accuracy) and reaction time. The stimuli were arranged in eight 30-s blocks with one block of the control condition alternating with one block of the WM condition.

Table 1. Demographics and Performance in the *DRD2* rs1076560 Genotype Groups

	GG	GT	Difference
<i>N</i>	18	10	
Age (y)	24.3 ± 3.1	22.8 ± 3.2	<i>df</i> = 26, <i>t</i> = 1.24, <i>P</i> = .23
Gender Ratio (M:F)	10:8	4:6	<i>df</i> = 1, <i>P</i> = .43
Hollingshead	41.9 ± 16.9	36.6 ± 11.6	<i>df</i> = 26, <i>t</i> = 0.89, <i>P</i> = .38
Wechsler Adult Intelligence Scale ^a (mean ± SEM)	113.1 ± 3.47	103.8 ± 6.38	<i>df</i> = 24, <i>t</i> = 1.38, <i>P</i> = .18
2-Back accuracy (% correct, mean ± SEM)	81.5 ± 3.37	88.2 ± 4.88	<i>df</i> = 26, <i>t</i> = 1.15, <i>P</i> = .26
2-Back Reaction Time (ms, mean ± SEM)	512.5 ± 51.65	562.1 ± 91.61	<i>df</i> = 26, <i>t</i> = 0.512, <i>P</i> = .63

^aAvailable for 24 subjects.

SPECT Imaging Acquisition

Each subject was injected intravenously with an average of 150 MBq (range 111–186 MBq) of available [¹²³I]-N-omega-fluoropropyl-2β-carbomethoxy-3β-(4-iodophenyl) tropane ([¹²³I]-FP-CIT; GE Healthcare, Amersham, UK), a radiotracer which binds specifically to DA transporters.³⁰ Potassium iodide solution (Lugol) was administered at least 3 h before and 12 h after radiopharmaceutical injection to block thyroid uptake of free radioactive iodide. Images were acquired 3–6 h after [¹²³I]-FP-CIT injection. A dual-head gamma camera (Infinia, GE) equipped with parallel-hole, low-energy high-resolution collimators was used. SPECT data were acquired using the following parameters: matrix = 128 × 128, rotation = 360°, view = 60, view angle = 6°, projection time = 45 s; slice thickness = 3.68 mm, acquisition time = 22 min; total brain counts >1 million in all examinations. Reconstruction was performed by back projection with a Butterworth filter (cutoff frequency: 0.3 cycle/cm, 10th order) to provide transaxial slices that were attenuation corrected. Attenuation correction was performed according to Chang's method (attenuation coefficient: 0.12–1 cm), after manually drawing an ellipse around the head contour. System spatial resolution was 11 mm (radius-of-rotation = 15.9 cm). Slices were reoriented parallel to the canthomeatal line.

Data Analysis

Behavioral and Demographics. Two-sample *t*-tests were used to compare demographics and behavioral data, respectively. Chi-square analyses were performed to compare categorical variables.

fMRI Imaging

Independent Component Analysis. One-group spatial independent component analysis (ICA) was performed on fMRI data preprocessed using Statistical Parametrical Mapping (SPM5; <http://www.fil.ion.ucl.ac.uk>) as implemented in Group ICA of fMRI Toolbox (GIFT2.0c; <http://icatb.sourceforge.net>) as described elsewhere³³ (see supplementary materials for further details). ICA decomposition was performed using the Infomax algorithm and

resulted in 21 independent components (ICs), consisting of group spatial maps and the related time courses (TCs) of the estimated signal. Individual participants' spatial maps for each IC, which are the voxel-wise IC loadings, represent local strength of functional connectivity^{31,32} and reflect the correspondence between the estimated TC in each voxel and the average TC of the network itself. Given that in spatial ICA, the individual subject TC is assumed to be constant across the entire brain, the voxel-wise estimated signal deviations from the average network reflects regional variation in the strength of functional connectivity within a given network. After screening for reliability, ICs with high spatial correlation ($R^2 > .02$ with the DMN template provided with the GIFT) were selected for further analyses as components of interest (COI). To further confirm the identification of selected COIs, we calculated Pearson's *r* correlation between their TCs and the 2-back condition (as modeled by a boxcar function convolved with a double-Gaussian hemodynamic response function) and retained those ICs that showed high temporal anticorrelation. We identified also a striatal COI with the highest spatial correlation ($R^2 = .07$) to an a priori defined bilateral basal ganglia (BG) region of interest (ROI, see below).

Second-Level Analyses. Each subject's COIs were entered into SPM5 and analyzed using second-level random-effects analyses. One-way ANOVAs, masked by the main effects maps of DMN-COIs for all the subjects ($P < .001$), with *DRD2* polymorphism as between-subjects variable were used to assess the effect of genotype on brain connectivity. Average connectivity strength as measured by individual subject IC loadings was extracted from significant clusters and correlated with V3'' in the BG within each genotype group (see below) using Spearman's ρ , thus yielding a total of 8 comparisons. Correlations were then compared using *r*-to-*z*' transform.

To study the relationship between *DRD2*-dependent connectivity differences in striatal network and DMN, we correlated connectivity strength between the clusters of networks that demonstrated *DRD2* genotype effects (MPFC and PCC, dorsal and ventral striatum, in DMN and striatal network, respectively) using Pearson's method

across the whole sample, thus yielding a total of 4 comparisons. Given the relatively large sample size ($n \geq 25$), here we used parametric statistics (Central Limit Theorem).

Clusters of contiguous voxels were identified using a statistical threshold of $P < .005$ uncorrected at voxel level. Then, these clusters were tested for cluster-level family-wise error correction for multiple comparisons with $\alpha = .05$ using Gaussian Random Field Theory. We corrected using the whole-brain volume or used small-volume correction for ROIs about which we had a priori hypotheses (anterior and posterior DMN regions and BG ROI). ROIs were created using WFU PickAtlas 1.04 (<http://www.rad.wfubmc.edu/fmri>). BG ROI comprised bilaterally the following brain regions: caudate, putamen, and globus pallidus. The DMN template was part of the GIFT toolbox and included the following regions: MPFC, anterior cingulate cortex (BA24/32), and the inferior parietal lobule, as well as the posterior cingulate and precuneus.¹ All coordinates are reported in Montreal Neurological Institute (MNI) system.

Temporal Analyses To evaluate DRD2-related differences in the engagement of the COIs across the whole task, we compared the beta values of the temporal correlations of each individual TC with the timing of each task condition using two-sample t tests as implemented in GIFT.³³

SPECT Imaging

Preprocessing. SPECT data were processed using SPM5 as previously reported.²⁹ For each subject, a specific-tonon displaceable equilibrium partition map (V3"), which is proportional to free voxel-wise DAT binding potential, was calculated (see supplementary materials).

Statistical Analyses. [¹²³I]-FP-CIT V3" data were extracted in each subject from a BG ROI, which included bilateral caudate and putamen (from WFU PickAtlas). V3" data were compared using a two-sample t -test. We performed an outlier analysis on the FP-CIT binding measures for the whole sample using the 1.5 \times interquartile range method.³⁴ According to this method, the 3 highest binding values (belonging to GG subjects) can be considered statistical outliers for the whole sample. We excluded these values from the SPECT analyses here reported. Nevertheless, all correlations between binding and connectivity remained unchanged when including these values (see supplementary materials), thus suggesting that those values are rather statistical albeit not biological outliers.

Results

Genotype Results

The allelic distribution of both genes was in Hardy-Weinberg equilibrium (DRD2, $\chi^2_1 = 1.323$, $P > .2$; DAT-VNTR,

$\chi^2_1 = 1.14$, $P > .2$). Furthermore, the distribution of DAT-VNTR did not differ across DRD2 groups ($\chi^2_1 = .208$; $P = .65$).

Behavioral Results

Genotype groups did not have any difference on both behavioral accuracy (percent correct responses: GG = 81.5 ± 14.3 , GT = 88.2 ± 15.4 ; $t_{26} = 1.154$, $P = .26$) and reaction time at 2-Back WM task (GG = 512.5 ± 219.1 milliseconds, GT = 562.1 ± 289.7 milliseconds; $t_{26} = 0.5116$, $P = .61$).

Imaging Results

Components of Interests. Consistent with previous fMRI studies,⁶ 2 DMN COIs were identified. The first COI encompassed brain regions that were more anterior (Ant-DMN, figure 1A) and included the MPFC (BA9/10), anterior cingulate (BA24/32), bilaterally hippocampal formation, and superior temporal and inferior parietal regions. The second COI included regions that were more posterior (post-DMN, figure 1B), as PCC (BA29/31), precuneus (BA5/7), posterior parietal cortex (BA7), and dorsal MPFC (BA10). Both COIs had high spatial correlation with the DMN template (Ant-DMN, $R^2 = .05$; post-DMN, $R^2 = .06$) as well as high temporal anti-correlation with the WM task (Ant-DMN, $r = -.73$, $P < .0001$; post-DMN, $r = -.80$, $P < .0001$).

The IC with the highest spatial correlation with BG ROI ($R^2 = .07$) was identified and labeled as striatal network. This COI encompassed bilaterally caudate, putamen, globus pallidus, ventral striatum, left dorsolateral-PFC (BA9), left supplementary motor area, and right superior posterior parietal cortex (figure 2). Also, this IC was anti-correlated with the WM condition ($r = -.54$, $P < .0001$).

Effect of DRD2 Genotype on Connectivity

There was an effect of genotype on Ant-DMN, post-DMN, and striatal networks. GG subjects had increased connectivity in MPFC relative to GT subjects within Ant-DMN (BA9/24; $xyz = -8, 53, 15$; $Z = 3.55$, $P = .03$ SVC corrected; figure 3A). In post-DMN, GG subjects had decreased connectivity in PCC relative to GT subjects (BA29/31; $xyz = 0, -34, 30$; $Z = 2.90$, $P = .04$ SVC corrected; figure 3A).

Within striatal network, GG subjects had greater connectivity in right ventral striatum relative to GT subjects ($xyz = 8, 4, -11$; $Z = 4.74$, $P = .05$ corrected, figure 4). Moreover, heterozygote subjects had greater connectivity in left putamen ($xyz = -30, -7.5, 0$; $Z = 3.13$, $P = .02$ SVC corrected for the striatum; figure 4).

Brain Network Correlations We investigated the relationship between connectivity strength, measured by IC loadings, in clusters demonstrating a DRD2 genotype effect, namely MPFC, PCC, right ventral striatum, and left putamen. In addition, there was a negative correlation between average spatial IC loadings in MPFC and PCC

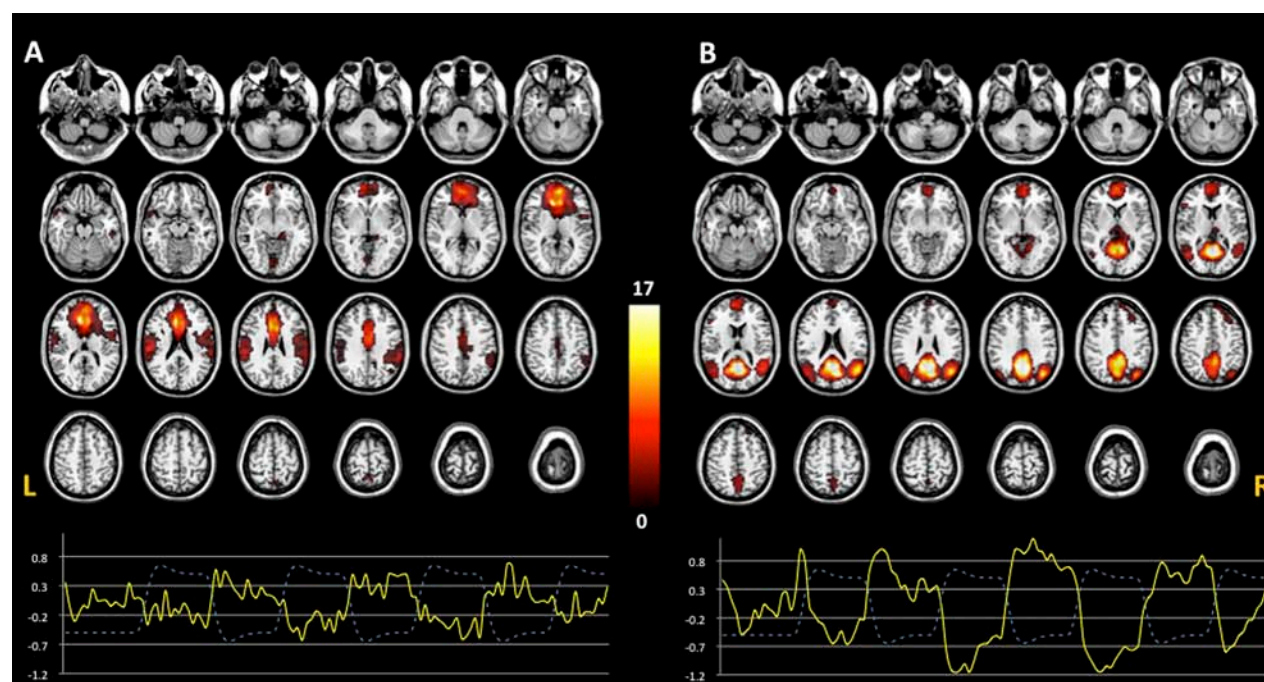


Fig. 1. Default mode network (DMN). Two components were identified: Ant-DMN (A) and post-DMN (B). The anterior component included MPFC, anterior cingulate, hippocampal formation, and superior temporal and inferior parietal regions, whereas the posterior component encompassed PCC, precuneus, dorsal MPFC, and bilateral posterior parietal regions. One sample *t* test images display the spatial pattern of the ICs identified ($P < .005$ uncorrected). TC represents the temporal profile of DMN for each component (continuous line) overlaid on the paradigm of working memory design (dashed line). Color bar indicates *T*-scores.

clusters across the whole sample ($r = -.40$, $P = .035$), such that subjects with lower engagement of MPFC within Ant-DMN had greater recruitment of PCC within post-DMN. There was a positive correlation between connectivity strength in the MPFC cluster within DMN and in ventral striatum within the striatal network ($r = .38$, $P = .045$; see supplementary figure S1A). Also, connectivity strength in PCC within post-DMN was correlated with connectivity in left putamen ($r = .43$, $P = .021$; see supplementary figure S1B).

SPECT Results

There was no statistically significant effect of genotype on $V3''$ values even though the direction of DAT binding in the 2 *DRD2* genotype groups was similar to what described before²⁹ (mean \pm standard error of the mean: GG = 2.98 ± 0.28 , GT = 2.38 ± 0.07 ; $t = 2.05$, $P > .2$).

Connectivity- $[^{123}\text{I}]\text{-FP-CIT } V3''$ Correlations

The relationship between connectivity in MPFC and $[^{123}\text{I}]\text{-FP-CIT}$ binding in BG was modulated by genotype ($P = .05$, figure 3B). In particular, IC loadings in MPFC were directly correlated with $[^{123}\text{I}]\text{-FP-CIT}$ binding in GG subjects ($\rho = 0.54$, $P = .038$), while in GT individuals, there was no significant correlation (the relationship was in the opposite direction, $\rho = -0.32$, $P = .36$).

Also, the relationship between connectivity in ventral striatum and $[^{123}\text{I}]\text{-FP-CIT}$ binding in the striatum was modulated by genotype ($P = .04$, see supplementary figure S2). Specifically, IC loadings were negatively correlated with $[^{123}\text{I}]\text{-FP-CIT}$ binding in GT subjects ($\rho = -0.64$, $P = .04$) while no significant correlation emerged in GG subjects (the relationship was again in the opposite direction, $\rho = 0.22$, $P = .37$). All statistics of the correlations did not change when including the possible statistical outliers (see supplementary figures S3 and S4).

Temporal Analyses

We found an effect of *DRD2* genotype on the beta values of striatal COI TC-task condition synchrony (all $P < .04$), with GT subjects having greater beta values relative to GG subjects.

Discussion

The present study demonstrates that *DRD2 rs1076560* genotype modulates connectivity within DMN along with its relationship with striatal $[^{123}\text{I}]\text{-FP-CIT}$ binding. Moreover, we found that *DRD2*-dependent DMN connectivity strength was correlated with *DRD2* genotype-dependent striatal connectivity. Specifically, GG subjects had greater connectivity in MPFC within Ant-DMN and

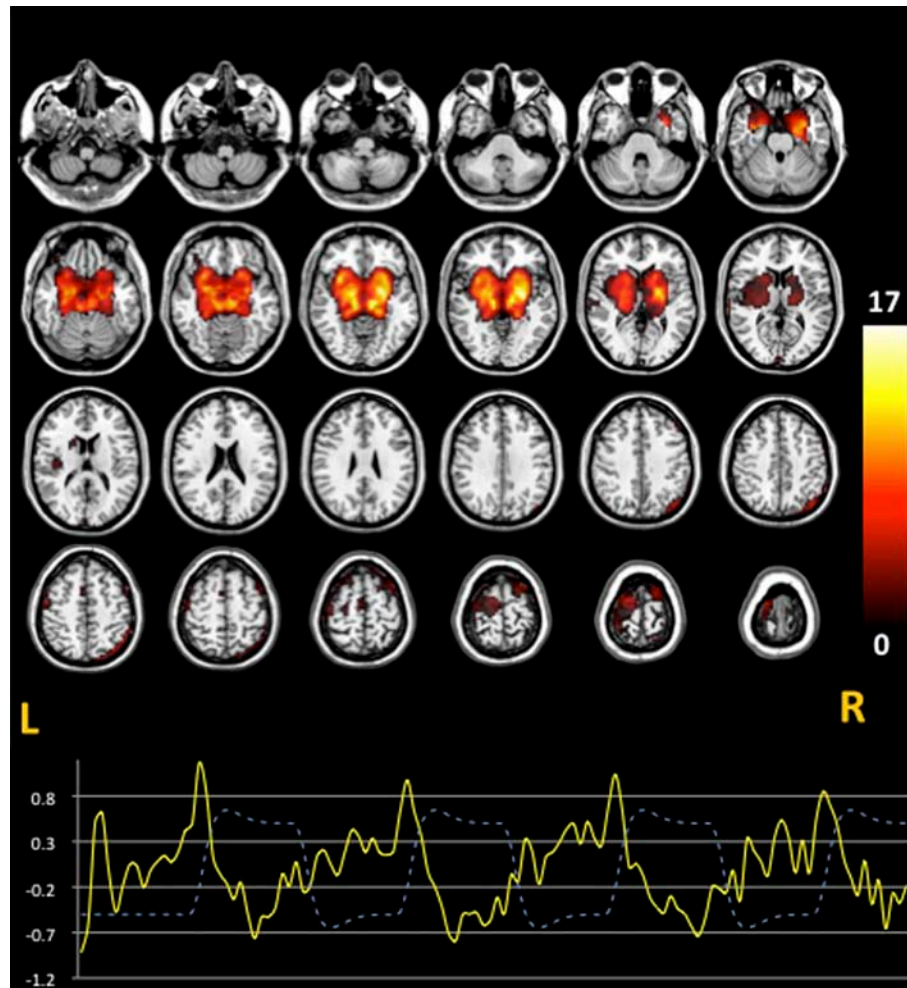


Fig. 2. The striatal network. A striatal component including caudate, putamen, pallidus, left dorsolateral PFC, and right superior posterior parietal cortex was estimated. One sample *t* test images display the spatial pattern of the ICs identified ($P < .005$ uncorrected). TC represents the temporal profile of the striatal network component (continuous line) overlaid on the paradigm of working memory design (dashed line). Color bar indicates *T*-scores.

decreased connectivity in PCC within post-DMN relative to GT subjects. Within the striatal network, connectivity strength in GG subjects was increased in ventral and reduced in dorsal striatum relative to GT subjects. Additionally, connectivity strength in ventral striatum and in MPFC as well as connectivity strength in dorsal striatum and in PCC were directly correlated. Furthermore, striatal [123 I]-FP-CIT binding was directly correlated with MPFC connectivity in GG subjects whereas this binding index was negatively correlated with ventral striatal connectivity in GT subjects.

Imaging genetics, pharmacological, and clinical studies in humans have indicated a modulatory role of DA signaling on both MPFC and PCC nodes within DMN at rest^{4,15} as well as during a cognitive task.^{8–12,16–18} Although most studies suggest that higher DA levels are associated with greater DMN activity, midline regions within this network show different responses to dopami-

nergic drugs^{9,10} or to genetic variants.¹⁶ In our study, we found regional *DRD2*-dependent changes in connectivity which may reflect both DA availability and anatomical-functional differences within the DMN. Presynaptic D2 autoreceptors (mainly D2S), which are relatively more abundant in GG subjects, inhibit DA release in the striatum.³⁵ Relatively decreased striatal DA signaling can result in increased PFC connectivity directly on frontal cortical neurons or through inhibitory interneurons (see, for a review, Tisch et al³⁶). Furthermore, the DMN includes different subnetworks with specific functional roles. MPFC, which is mainly connected with limbic regions such as the orbitofrontal cortex,³⁷ has been implicated in emotional processing and motivation.³⁸ Also, MPFC can filter out interference from emotional processing that may hamper performance during cognitive tasks in a dynamic interplay with the task-related network.³⁹ Overall, these reports support a role for this

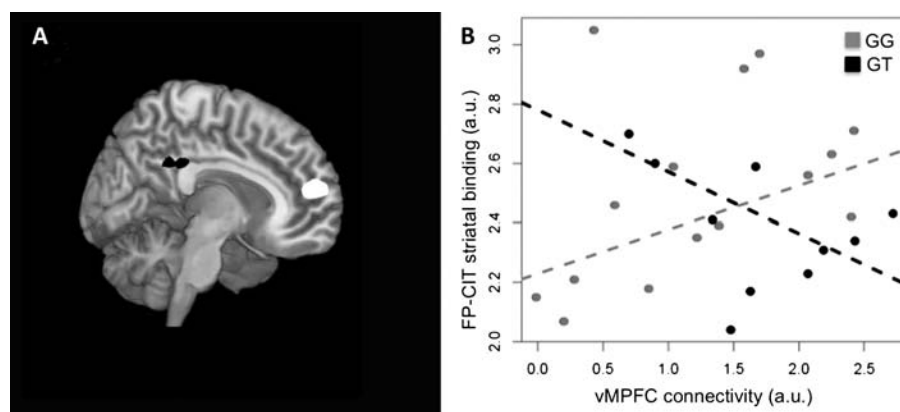


Fig. 3. Effect of *DRD2* rs1076560 on functional connectivity within the DMN. (A) GG subjects had greater connectivity strength within the Ant-DMN in MPFC relative to GT subjects (white cluster [shown in green in online version]); GG subjects had reduced connectivity in PCC within post-DMN (black cluster [shown in red in online version]) relative to GT subjects. (B) Connectivity in MPFC correlated with striatal FP-CIT binding in GG ($\rho = 0.54$, $P = .04$) but not in GT subjects ($\rho = -0.32$, $P = .36$). T-map of DMN connectivity differences are thresholded at $P = .005$ and overlaid on the MNI brain template for visual purposes. (white [green in online version], GG > GT; black [red in online version], GT > GG).

region in monitoring and integrating emotional and cognitive processing.² On the other hand, PCC is connected with the anterior cingulate cortex, the parietal cortex, and the hippocampus. PCC activity has been associated with difficulty of cognitive tasks⁶ and with both short and

long-term memory processing.⁴⁰ We found that GG subjects have greater connectivity in MPFC and reduced connectivity in PCC in the context of comparable accuracy and reaction time at the task at hand. Previous reports have indicated that healthy GG subjects have better performance at cognitive tasks and decreased dorsolateral PFC activation in the context of similar accuracy.^{28,29} On the other hand, GG subjects have reduced emotional control and increased amygdala activation during implicit processing of emotional faces along with greater dorsolateral-PFC response in explicit processing.²² Hence, increased connectivity in the anterior DMN and decreased connectivity in the posterior DMN, respectively, may reflect a general capacity of these individuals to preferentially engage specific nodes in these networks associated with differential behavioral abilities.

Functional activity in the striatum is modulated by *DRD2* genotype variants during WM^{27,28} and motor tasks.⁴¹ The striatal network has been identified by previous studies^{42,43} and may include sensory-motor, cognitive and limbic loops. Interestingly, the hemodynamic response of the striatal network was shown to precede that of the DMN during resting state, thus suggesting that the striatal network may function also as a controller of network fluctuations within the DMN.⁴³ Ventral striatal regions are associated with limbic function and receive glutamatergic projections from PFC, amygdala, and hippocampus, as well as DA fibers from ventral tegmental area. On the other hand, the dorsal striatum is associated with sensorimotor and cognitive function, receiving glutamatergic projections from the cortex and dopaminergic afferents from substantia nigra pars compacta (for a review, see Haber and Knutson⁴⁴). Striatal D2 receptors are abundantly expressed both presynaptically on DA terminals from the substantia nigra and PFC and postsynaptically

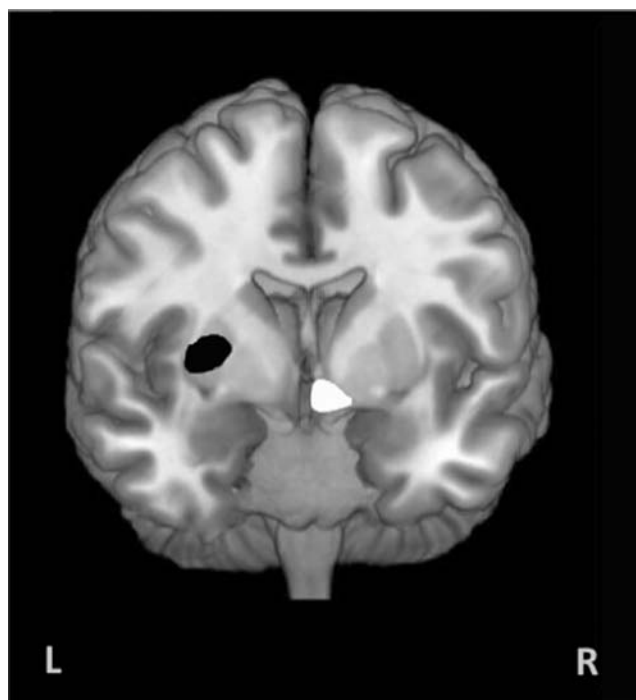


Fig. 4. Effect of *DRD2* rs1076560 on functional connectivity within the striatal network. (A) GG subjects had greater connectivity strength in right ventral striatum (white cluster [green in online version]) relative to GT subjects as well as reduced connectivity in left putamen (black cluster [red in online version]) relative to GT subjects. T-maps of striatal connectivity differences are thresholded at $P = .005$ and overlaid on the MNI brain template for visual purposes.

on γ -aminobutyric acid (GABA) medium spiny neurons.⁴⁵ We found that *DRD2* modulates the synchrony of the entire striatal network and the WM task, with GG subjects having decreased temporal correlation with the task. Furthermore, we found that in GG subjects, connectivity was increased in ventral striatum and reduced in dorsal striatum. These striatal changes may reflect the effects of genetic variation of *DRD2* on the relative distribution of D2 isoforms. Indeed, the ratio of striatal and PFC D2S/D2L isoforms may affect the balance between excitatory and inhibitory transmission in the striatum that ultimately regulates the firing of medium spiny neurons. The role of D2 isoform ratio in striatal connectivity is also supported by our SPECT results. Striatal D2S regulate DAT availability and DA levels that are the main factors associated with resting [¹²³I]-FP-CIT binding indexes.²³ In keeping with this, we found that [¹²³I]-FP-CIT binding predicts reduced ventral striatal connectivity in GT subjects further suggesting the role of D2S levels in striatal function.

The DMN is anatomically and functionally associated with brain regions within striatal networks. Evidence from functional connectivity research in humans^{13,46} and anatomical studies in non-human primates³⁷ have demonstrated that MPFC is connected to the ventral striatum. MPFC inputs to the striatum are organized in a dual system: focal projections to subregions of the ventral striatum, specifically to the nucleus accumbens, the medial portion of the caudate, and the ventromedial part of the putamen, which play a role in encoding the relative value and the outcome of chosen options during decisions⁴⁷; diffuse pathways to the entire striatum that converge with inputs from other PFC areas and regulate the firing of medium spiny neurons, thus modulating temporal activation of different striatal regions during learning.⁴⁸ Tracer studies in monkeys⁴⁹ and imaging studies⁴ have shown that the dorsal caudate is connected with PCC. Intriguingly, pharmacological challenge with DA agonists, and Positron Emission Tomography (PET) studies have shown that DA signaling can modulate the relationship between the DMN and striatal networks both at rest⁴ and during the performance of a cognitive task.¹⁷ We found that *DRD2*-dependent changes in ventral striatal connectivity within the striatal network and in MPFC connectivity within the DMN are associated, suggesting a modulatory role of D2 variants on the DMN-striatal network relationship. The role of genetic variation of D2S receptors is also suggested by the association between MPFC connectivity and [¹²³I]-FP-CIT striatal binding in GG subjects. Alternatively, DA levels per se can modulate the relationship between DMN and striatal networks. Resting PET studies with fluoro-L-tyrosine, a radiotracer which measures DA synthesis capacity, show that dorsal striatal binding can predict activity in PCC during a WM task.¹⁷ Consistent with these findings, GT subjects, who are thought to have greater striatal DA concentration, showed greater connectivity

in dorsal striatum. Furthermore, strength of connectivity in this region was associated with coupling in PCC.

These findings provide further evidence for an important role of the D2 system in the modulation of the DMN. The relative ratio of D2 isoforms can modulate both DA and GABA pathways. DA can modulate firing of pyramidal neurons and of GABA inhibitory interneurons through DA receptors including D2, thus affecting network synchronization of cortical oscillations.¹⁹ Furthermore, activity of DMN has been directly associated with decreases in neuronal activity due to inhibitory processes.⁵⁰ Both D2S and D2L can affect neural inhibition directly through modulation of tonic activity of GABAergic interneurons⁵¹ and indirectly through the inhibition of glutamate release (mainly D2S⁵²). Thus, modulation of cortical and striatal D2 systems could result in changes at the level of excitatory and inhibitory systems which translate in differential patterns of network engagement within the DMN.

Overall, these findings suggest that *DRD2* polymorphism can have pleiotropic effects on the DMN through the modulation of striatal DA. Levels of this neurotransmitter could affect functional coupling within regions of the DMN, the striatal network, and their interaction to modulate the dynamic interplay among brain networks.⁴ Coordinated interaction among cerebral circuits is thought to be crucial for the allocation of attentional resources during active and passive states where attention is directed towards a task or self-reflected respectively.⁶

Notably, dysregulation of DA and of the D2 pathway is thought to be crucial for the pathophysiology and treatment of schizophrenia. A number of studies support dysregulation of striatal DA and increased D2 striatal density in patients with schizophrenia (see, for a review, Abi-Dargham⁵³). Furthermore, imaging studies have reported that genetically determined D2 signaling is associated with dorsolateral-PFC activity during WM.^{23,27–29} Finally, the DMN contributes to WM function⁶ and is also altered in patients with schizophrenia.^{7,54} DMN anomalies in this brain disorder may be associated with altered D2 signaling¹⁶ and dysfunctional interactions with task-related networks.⁶ Altered D2 signaling, which may follow *DRD2*-genotype related differences in D2S/D2L expression ratio, can disrupt the DMN function.¹⁶ Disrupted dynamics of brain networks may impair the recruitment of attentional resources for goal-directed behavior and be associated with the cognitive symptoms of schizophrenia.⁷ Both typical and atypical antipsychotics, which have D2 antagonist properties, can modulate striatal activity increasing glutamate levels in the neocortex via corticostriatal projections as well as GABAergic activity (see above). These neural changes may translate at the level of brain systems to increased functional connectivity in the DMN.^{7,15}

A limitation to this study is the possible effect of task performance on the estimation of DMN connectivity per

se and on between-group comparisons. While the identification of ICs during a task has inherent advantages on the functional classification of the ICs, it may bias the temporal response of the estimated ICs relative to resting studies. In particular, the 2-back task anticorrelation of the striatal IC may have resulted as a consequence of task switching and motor processes during 0-back condition differently from resting state.⁴³ Nevertheless, recent imaging studies performed on thousands of subjects have confirmed the spatial consistency of the brain networks estimated using ICA during rest and during an active task.⁵⁵ Consistently, the spatial components identified in our study were similar to those previously identified by other groups.⁵⁵ Also, the lack of behavioral differences at the task across genotype groups further suggests that behavioral performance may have not biased our results. Another shortcoming of the present study was the presence of IQ differences between genotype groups (GG > GT). Although this difference was not significant, a bigger sample size might have revealed a role of *DRD2* genotype on IQ measures, and this effect could have mediated our results. Conversely, Zhang et al.²⁸, who studied 68 healthy controls, found that GT subjects had a relatively greater IQ, again this difference did not reach statistical significance. To further exclude a contribution of IQ differences on our results, we tested the correlation between imaging and behavioral data and IQ scores. We did not find any significant association.

Although our multimodal study included sample of 28 subjects, only a smaller number (10) of them had a GT genotype. This is consistent with the minor allele frequency reported for the T allele, which is between 0.1 and 0.2 in Caucasian populations. The exclusion of possible statistical outliers critically diminished our ability to detect *DRD2* binding differences across genotype groups which was reported in a larger sample.²⁹ Nevertheless, our study was sufficiently powered to detect significant differences in imaging variables across genotypes.

In conclusion, our findings indicate that genetic variation in *DRD2* modulates connectivity within the DMN. Our data also suggest that *DRD2* can modulate connectivity in the striatum, and these changes are associated with differences in the engagement of the DMN. Further studies are needed to ascertain the relevance of the modulation of DMN and striatal networks by DA pathways in neuropsychiatric disorders.

Supplementary Material

Supplementary figures S1–S4 and other materials are available at <http://schizophreniabulletin.oxfordjournals.org>.

Funding

Marie Curie Reintegration Grant (FP7-276981) to F.S.

Acknowledgment

We would like to acknowledge Riccarda Lomuscio for help with data acquisition.

References

1. Raichle ME, MacLeod AM, Snyder AZ, Powers WJ, Gusnard DA, Shulman GL. A default mode of brain function. *Proc Natl Acad Sci U S A*. 2001;98:676–682.
2. Andrews-Hanna JR, Reidler JS, Sepulcre J, Poulin R, Buckner RL. Functional-anatomic fractionation of the brain's default network. *Neuron*. 2010;65:550–562.
3. Di Martino A, Scheres A, Margulies DS, et al. Functional connectivity of human striatum: a resting state FMRI study. *Cereb Cortex*. 2008;18:2735–2747.
4. Kelly C, de Zubicaray G, Di Martino A, et al. L-dopa modulates functional connectivity in striatal cognitive and motor networks: a double-blind placebo-controlled study. *J Neurosci*. 2009;29:7364–7378.
5. Gusnard DA, Akbudak E, Shulman GL, Raichle ME. Medial prefrontal cortex and self-referential mental activity: relation to a default mode of brain function. *Proc Natl Acad Sci U S A*. 2001;98:4259–4264.
6. Sambataro F, Murty VP, Callicott JH, et al. Age-related alterations in default mode network: impact on working memory performance. *Neurobiol Aging*. 2010;31:839–852.
7. Sambataro F, Blasi G, Fazio L, et al. Treatment with olanzapine is associated with modulation of the default mode network in patients with Schizophrenia. *Neuropsychopharmacology*. 2010;35:904–912.
8. Nagano-Saito A, Liu J, Doyon J, Dagher A. Dopamine modulates default mode network deactivation in elderly individuals during the Tower of London task. *Neurosci Lett*. 2009;458:1–5.
9. Argyelan M, Carbon M, Ghilardi MF, et al. Dopaminergic suppression of brain deactivation responses during sequence learning. *J Neurosci*. 2008;28:10687–10695.
10. Tomasi D, Volkow ND, Wang GJ, et al. Methylphenidate enhances brain activation and deactivation responses to visual attention and working memory tasks in healthy controls. *Neuroimage*. 2011;54:3101–3110.
11. Min. zenberg MJ, Yoon JH, Carter CS. Modafinil modulation of the default mode network. *Psychopharmacology (Berl)*. 2011;215:23–31.
12. Nagano-Saito A, Leyton M, Monchi O, Goldberg YK, He Y, Dagher A. Dopamine depletion impairs frontostriatal functional connectivity during a set-shifting task. *J Neurosci*. 2008;28:3697–3706.
13. van Eimeren T, Monchi O, Ballanger B, Strafella AP. Dysfunction of the default mode network in Parkinson disease: a functional magnetic resonance imaging study. *Arch Neurol*. 2009;66:877–883.
14. Delaveau P, Salgado-Pineda P, Fossati P, Witjas T, Azulay JP, Blin O. Dopaminergic modulation of the default mode network in Parkinson's disease. *Eur Neuropsychopharmacol*. 2010;20:784–792.
15. Liu B, Song M, Li J, et al. Prefrontal-related functional connectivities within the default network are modulated by COMT val158met in healthy young adults. *J Neurosci*. 2010;30:64–69.
16. Stokes PR, Rhodes RA, Grasby PM, Mehta MA. The effects of the COMT val(108/158)met polymorphism on BOLD

- activation during working memory, planning, and response inhibition: a role for the posterior cingulate cortex? *Neuropsychopharmacology*. 2011;36:763–771.
17. Braskie MN, Landau SM, Wilcox CE, et al. Correlations of striatal dopamine synthesis with default network deactivations during working memory in younger adults. *Hum Brain Mapp*. 2011;32:947–961.
18. Tomasi D, Volkow ND, Wang R, et al. Dopamine transporters in striatum correlate with deactivation in the default mode network during visuospatial attention. *PLoS One*. 2009;4:e6102.
19. Seamans JK, Yang CR. The principal features and mechanisms of dopamine modulation in the prefrontal cortex. *Prog Neurobiol*. 2004;74:1–58.
20. Kimberg DY, Aguirre GK, Lease J, D'Esposito M. Cortical effects of bromocriptine, a D-2 dopamine receptor agonist, in human subjects, revealed by fMRI. *Hum Brain Mapp*. 2001;12:246–257.
21. Mehta MA, Montgomery AJ, Kitamura Y, Grasby PM. Dopamine D2 receptor occupancy levels of acute sulpiride challenges that produce working memory and learning impairments in healthy volunteers. *Psychopharmacology (Berl)*. 2008;196:157–165.
22. Blasi G, Lo Bianco L, Taurisano P, et al. Functional variation of the dopamine D2 receptor gene is associated with emotional control as well as brain activity and connectivity during emotion processing in humans. *J Neurosci*. 2009;29:14812–14819.
23. Bertolino A, Fazio L, Caforio G, et al. Functional variants of the dopamine receptor D2 gene modulate prefronto-striatal phenotypes in schizophrenia. *Brain*. 2009;132(pt 2):417–425.
24. Blasi G, Napolitano F, Ursini G, et al. DRD2/AKT1 interaction on D2 c-AMP independent signaling, attentional processing, and response to olanzapine treatment in schizophrenia. *Proc Natl Acad Sci U S A*. 2011;108:1158–1163.
25. Lee FJ, Pei L, Moszczynska A, Vukusic B, Fletcher PJ, Liu F. Dopamine transporter cell surface localization facilitated by a direct interaction with the dopamine D2 receptor. *EMBO J*. 2007;26:2127–2136.
26. Bolan EA, Kivell B, Jalgam V, et al. D2 receptors regulate dopamine transporter function via an extracellular signal-regulated kinases 1 and 2-dependent and phosphoinositide 3 kinase-independent mechanism. *Mol Pharmacol*. 2007;71:1222–1232.
27. Bertolino A, Fazio L, Di Giorgio A, et al. Genetically determined interaction between the dopamine transporter and the D2 receptor on prefronto-striatal activity and volume in humans. *J Neurosci*. 2009;29:1224–1234.
28. Zhang Y, Bertolino A, Fazio L, et al. Polymorphisms in human dopamine D2 receptor gene affect gene expression, splicing, and neuronal activity during working memory. *Proc Natl Acad Sci U S A*. 2007;104:20552–20557.
29. Bertolino A, Taurisano P, Pisciotto NM, et al. Genetically determined measures of striatal D2 signaling predict prefrontal activity during working memory performance. *PLoS One*. 2010;5:e9348.
30. Scherfler C, Seppi K, Donnemiller E, et al. Voxel-wise analysis of [123I]beta-CIT SPECT differentiates the Parkinson variant of multiple system atrophy from idiopathic Parkinson's disease. *Brain*. 2005;128(pt 7):1605–1612.
31. Beckmann CF, DeLuca M, Devlin JT, Smith SM. Investigations into resting-state connectivity using independent component analysis. *Philos Trans R Soc Lond B Biol Sci*. 2005;360:1001–1013.
32. van de Ven VG, Formisano E, Prvulovic D, Roeder CH, Linden DE. Functional connectivity as revealed by spatial independent component analysis of fMRI measurements during rest. *Hum Brain Mapp*. 2004;22:165–178.
33. Sambataro F, Reed JD, Murty VP, et al. Catechol-O-methyltransferase valine(158) methionine polymorphism modulates brain networks underlying working memory across adulthood. *Biol Psychiatry*. 2009;66:540–548.
34. Barnett V, Lewis T. *Outliers in Statistical Data*. 2nd ed. New York, NY: John Wiley & Sons; 1985.
35. Watanabe K, Kita T, Kita H. Presynaptic actions of D2-like receptors in the rat cortico-striato-globus pallidus disynaptic connection in vitro. *J Neurophysiol*. 2009;101:665–671.
36. Tisch S, Silberstein P, Limousin-Dowsey P, Jahanshahi M. The basal ganglia: anatomy, physiology, and pharmacology. *Psychiatr Clin North Am*. 2004;27:757–799.
37. Ongur D, Price JL. The organization of networks within the orbital and medial prefrontal cortex of rats, monkeys and humans. *Cereb Cortex*. 2000;10:206–219.
38. Groenewegen HJ, Uylings HB. The prefrontal cortex and the integration of sensory, limbic and autonomic information. *Prog Brain Res*. 2000;126:3–28.
39. Longe O, Senior C, Rippon G. The lateral and ventromedial prefrontal cortex work as a dynamic integrated system: evidence from FMRI connectivity analysis. *J Cogn Neurosci*. 2009;21:141–154.
40. Kobayashi Y, Amaral DG. Macaque monkey retrosplenial cortex: II. Cortical afferents. *J Comp Neurol*. 2003;466:48–79.
41. Fazio L, Blasi G, Taurisano P, et al. D2 receptor genotype and striatal dopamine signaling predict motor cortical activity and behavior in humans. *Neuroimage*. 2011;54:2915–2921.
42. Damoiseaux JS, Beckmann CF, Arigita EJ, et al. Reduced resting-state brain activity in the “default network” in normal aging. *Cereb Cortex*. 2008;18:1856–1864.
43. Robinson S, Basso G, Soldati N, et al. A resting state network in the motor control circuit of the basal ganglia. *BMC Neurosci*. 2009;10:137.
44. Haber SN, Knutson B. The reward circuit: linking primate anatomy and human imaging. *Neuropsychopharmacology*. 2010;35:4–26.
45. Lindgren N, Usiello A, Gojny M, et al. Distinct roles of dopamine D2L and D2S receptor isoforms in the regulation of protein phosphorylation at presynaptic and postsynaptic sites. *Proc Natl Acad Sci U S A*. 2003;100:4305–4309.
46. Greicius MD, Krasnow B, Reiss AL, Menon V. Functional connectivity in the resting brain: a network analysis of the default mode hypothesis. *Proc Natl Acad Sci U S A*. 2003;100:253–258.
47. Luk CH, Wallis JD. Dynamic encoding of responses and outcomes by neurons in medial prefrontal cortex. *J Neurosci*. 2009;29:7526–7539.
48. Kasanetz F, Riquelme LA, Della-Maggiore V, O'Donnell P, Murer MG. Functional integration across a gradient of corticostriatal channels controls UP state transitions in the dorsal striatum. *Proc Natl Acad Sci U S A*. 2008;105:8124–8129.
49. Kunishio K, Haber SN. Primate cingulo-striatal projection: limbic striatal versus sensorimotor striatal input. *J Comp Neurol*. 1994;350:337–356.

50. Shmuel A, Yacoub E, Pfeuffer J, et al. Sustained negative BOLD, blood flow and oxygen consumption response and its coupling to the positive response in the human brain. *Neuron*. 2002;36:1195–1210.
51. Janssen MJ, Ade KK, Fu Z, Vicini S. Dopamine modulation of GABA tonic conductance in striatal output neurons. *J Neurosci*. 2009;29:5116–5126.
52. Centonze D, Grande C, Usiello A, et al. Receptor subtypes involved in the presynaptic and postsynaptic actions of dopamine on striatal interneurons. *J Neurosci*. 2003;23:6245–6254.
53. Abi-Dargham A. Do we still believe in the dopamine hypothesis? New data bring new evidence. *Int J Neuropsychopharmacol*. 2004;7(suppl 1):S1–S5.
54. Salgado-Pineda P, Fakra E, Delaveau P, McKenna PJ, Pomarol-Clotet E, Blin O. Correlated structural and functional brain abnormalities in the default mode network in schizophrenia patients. *Schizophr Res*. 2011;125:101–109.
55. Smith SM, Fox PT, Miller KL, et al. Correspondence of the brain's functional architecture during activation and rest. *Proc Natl Acad Sci U S A*. 2009;106:13040–13045.